Supplementary Information (SI) for Nanoscale.

Supporting Information

Microbe-Mediated Synthesis of Defect-rich CeO_2 Nanoparticles with Oxidase-like Activity for Colorimetric Detection of L–penicillamine and Glutathione

Nan Zhang[a], Yingyan Du[a], Zhidong Zhang[d], Liying Zhu[a,], Ling Jiang[b,c]*

[a]School of Chemistry and Molecular Engineering, Nanjing Tech University, Nanjing 211816, P. R. China

[b]College of Biotechnology and Pharmaceutical Engineering, State Key Laboratory of Materials-Oriented Chemical Engineering, Nanjing Tech University, Nanjing 211816, P. R. China

[c]College of Food Science and Light Industry, Nanjing Tech University, Nanjing 211816, P. R. China

[d]Xinjiang Key Laboratory of Special Environmental Microbiology, Institute of Applied Microbiology, Xinjiang Academy of Agricultural Sciences, Xinjiang 830091, P. R. China

***Corresponding Author**

E-mail: zlyhappy@njtech.edu.cn

Contents

Experimental Section

Reagents and materials.

Ultrapure water was homemade and used in all experiments in the case of no additional instructions. Cerium(III) Acetate Hydrate ($(CH_3CO_2)_3Ce{\cdot}xH_2O$, 99.99%), 3,3′,5,5′–tetramethylbenzidine (TMB, 99%), cerium(IV) sulfate ($Ce(SO_4)_2$, 99.95%), EDTA-2Na (98%), histidine (98%), 1,4–benzochinon (*p*–BQ, 99%), thiourea (99%), fructose (99%), lactose (98%), L–lysine (98%), L–serine (99%), L–tryptophan (99%), D–phenylalanine (99%), L–valine (99%), L–isoleucine (99%) and goat Serum were purchased from Shanghai Titan Technology Co.,Ltd., China. L–penicillamine (L–PA, >98%), Glutathione (GSH, >98%), calcium Acetate ($Ca(CH_3COO)_2$, AR), magnesium acetate ($Mg(CH_3COO)_2$, 98%), potassium acetate (CH_3COOK, 99.9%), and galactose (98%) were purchased from Shanghai Macklin Biochemical Co.,Ltd., China. Sodium chloride (NaCl, AR), sodium sulfate (Na_2SO_4, AR), sodium carbonate (Na_2CO_3, AR), sodium acetate (CH_3COONa, AR), sodium bicarbonate ($NaHCO_3$, AR), glacial acetic acid (CH_3COOH, AR), glucose (AR), sucrose (AR), and ethanol (AR) were purchased from Sinopharm Group Co.,Ltd., China. All the chemicals were used without any further purification.

Characterization.

The morphology and structure were characterized by transmission electron microscope (TEM) (JEM-F200, JEOL, Japan). The high-resolution transmission electron microscope was used to obtain high-angle annular dark-field scanning transmission electron microscopy (HAADF-STEM) and element mapping images. The crystal structure was investigated by X-ray diffractometer (XRD) (MiniFlex600, Rigaku Corporation, Japan) in the scanning range of 2θ between 20° and 80° with copper Kα as the source of radiation. The surface chemical information was collected by X-ray photoelectron

spectroscopy (XPS) with Al-Kα X-ray source (K-Alpha, Thermo Scientific, USA). The phase structure of the materials were characterized by Raman spectroscopy with 532 nm laser excitation (DXR2, Thermo Fisher Scientific, USA). The electron paramagnetic resonance signals were obtained on electron paramagnetic resonance spectrometer (EPR, Bruker, EMXplus6/1, Germany).

Oxidase-like Catalytic Activity of CeO_2 NPs.

10 μL CeO_2 NPs (10 mg/mL) and 20 μL TMB (5 mM) were added into 970 μL 0.2 M NaAc/HAc buffer (pH = 3.8). Then the reaction solution was incubated in a metal bath at 50°C for 20 min, and finally cooled in an ice bath for 10 min. The OXD-like activity of CeO_2 NPs were evaluated by the optical density of the reaction solution at 652 nm or 400-800 nm in a Ultraviolet visible light (UV–vis) spectrophotometer (Lambda 25, PerkinElmer, USA).

Kinetic Measurements.

The steady-state kinetics measurement of CeO_2 NPs was carried out according to a general strategy. Briefly, the final concentration of TMB was varied (0.05–3 mM) in 0.2 M NaAc/HAc buffer (pH = 3.8) containing 10 μg/mL CeO_2 NPs, keeping the total volume of the reaction solution at 1 mL. The absorbance change at 652 nm was monitored for 3 min with a 20 s time interval in a UV–vis spectrophotometer (Lambda 25, PerkinElmer, USA) to obtain the initial velocities at different substrate concentrations. The Michaelis-Menten curve was obtained by fitting the initial velocity values and the substrate concentrations to the Michaelis-Menten equation as follows:

$$\frac{1}{V} = \frac{1}{V_{max}} + \frac{K_m}{V_{max}[S]}$$

Where V is the initial velocity, V_{max} represents the maximum reaction velocity, [S]

is the substrate concentration. The Michaelis-Menten constant (K_m) and V_{max} were calculated by a Line-Burk plot.

Detection of L–PA and GSH.

In the detection of L–PA, 10 μL CeO_2 NPs (10 mg/mL), 20 μL TMB (5 mM) and 40 μL L–PA solution with different concentrations (10–500 μM) were added into 930 μL 0.2 M NaAc/HAc buffer (pH = 3.8). Then the reaction solution was incubated in metal bath at 50°C for 20 min, and finally cooled in an ice bath for 10 min. Finally, the absorbance of the reaction solution at 652 nm or 400-800 nm was measured.

In the detection of GSH, 10 μL CeO_2 NPs (10 mg/mL) and 20 μL TMB (5 mM) were added into 870 μL 0.2 M NaAc/HAc buffer (pH = 3.8). After been incubated in metal bath at 50°C for 20 min 100 mL GSH solution with different concentrations (9–250 μM) were added and the mixture was immediately cooled in an ice bath for 10 min. Finally, the absorbance of the reaction solution at 652 nm or 400-800 nm was measured.

Selectivity study of the CeO_2–TMB system for the detection of L–PA and GSH.

Selectivity study of the CeO_2–TMB system for the detection of L–PA was performed by replacing 0.1 mM L–PA with 0.5 mM interfering substance (ampicillin sodium, K^+, Ca^{2+}, Na^+, Mg^{2+}, Cl, SO_4^{2-}, CO_3^{2-}, HCO_3^-, glucose, fructose, lactose, galactose, sucrose, lysine, serine, tryptophan, phenylalanine, valine and isoleucine).

Selectivity study of the CeO_2–TMB system for the detection of GSH was performed by replacing 0.05 mM GSH with 0.05 mM L–PA or 0.5 mM other interfering substance (K^+, Ca^{2+}, Na^+, Mg^{2+}, Cl^-, SO_4^{2-}, CO_3^{2-}, HCO_3^-, glucose, fructose, lactose, galactose, sucrose, lysine, serine, tryptophan, phenylalanine, valine and isoleucine).

Detection of L–PA and GSH in the Real Samples.

Tape water, lake water and goat serum were used as real samples in the detection of L–penicillamine. All water samples were taken from Nanjing Tech University. The samples were pretreated by centrifuging at 5000 rpm for 5 minutes and filtrating by 0.22 μm pore-size syringe filter. 10 μL CeO_2 NPs (10 mg/mL), 20 μL TMB (5 mM) and 40 μL sample solutions were added into 930 μL 0.2 M NaAc/HAc buffer (pH = 3.8). Then the reaction solution was incubated in metal bath at 50°C for 20 min, and finally cooled in an ice bath for 10 min. The absorbance of the reaction solution at 652 nm was measured.

Glutathione tablets were used as real samples in the detection of GSH. After careful grinding, 0.015 g of glutathione tablets were weighed and ultrasonically dispersed in 100 mL of deionized water. Then the solution was centrifuged at 5000rpm for 5 minutes, and the supernatant was filtered by 0.22 μm pore-size syringe filter. Finally, the filtrate was diluted 50 times with deionized water for use. 10 μL CeO_2 NPs (10 mg/mL) and 20 μL TMB (5 mM) were added into 870 μL 0.2 M NaAc/HAc buffer (pH = 3.8). Then the reaction solution was incubated in metal bath at 50°C for 20 min. After adding 100 μL samples, the mixture was immediately cooled in an ice bath for 10 min. Finally, the absorbance of the reaction solution at 652 nm was measured.

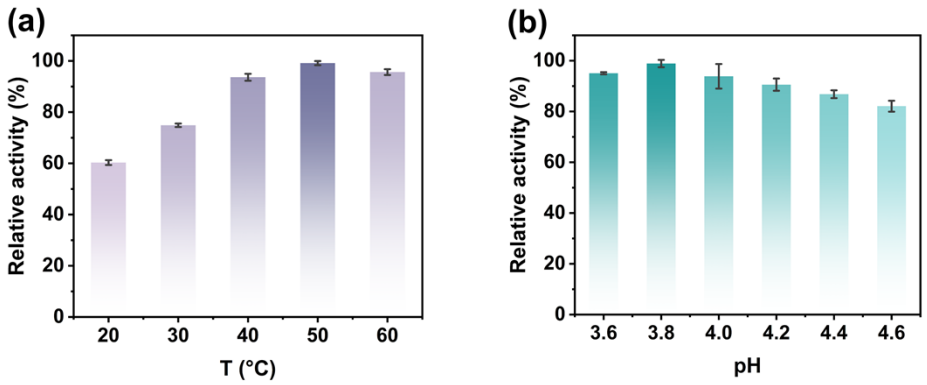

Figure S1. Effects of (a) reaction temperature and (b) system pH on the OXD-like activity of the biosynthesized CeO_2 NPs.

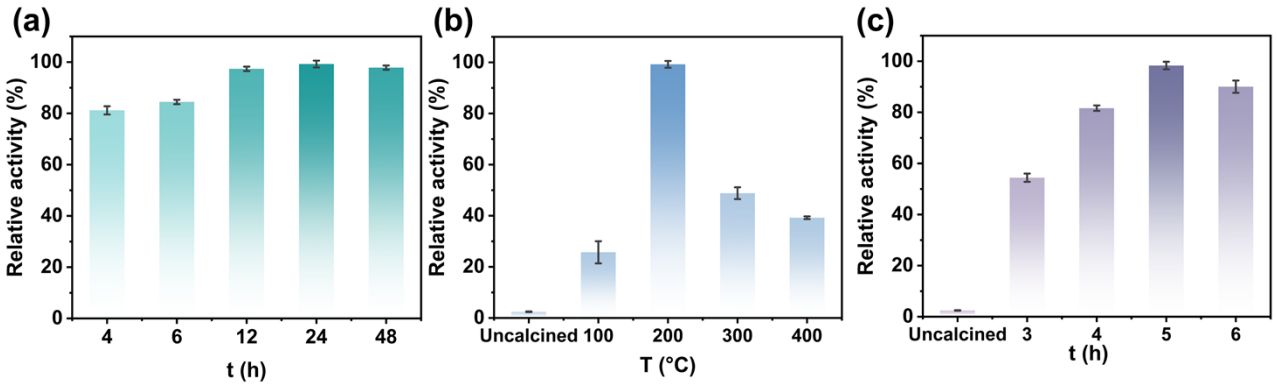

Figure S2. Effects of (a) incubate time, (b) calcination temperature, and (c) calcination time on the OXD-like activity of the biosynthesized CeO_2 NPs.

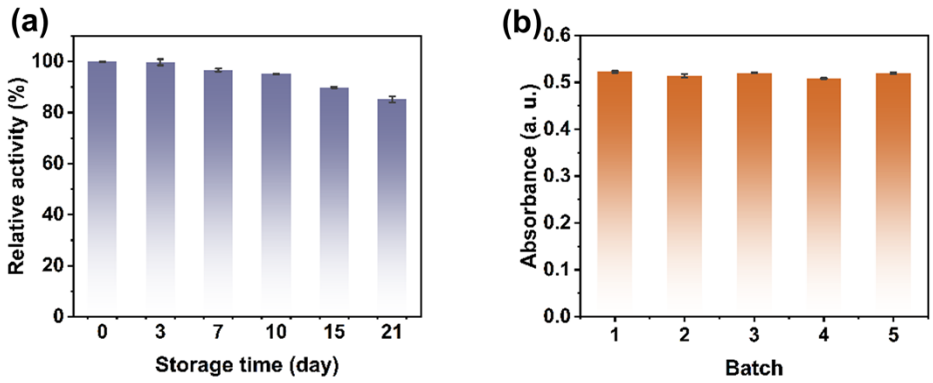

Figure S3. The (a) storage and (b) batch stability studies of the biosynthesized CeO_2 NPs.

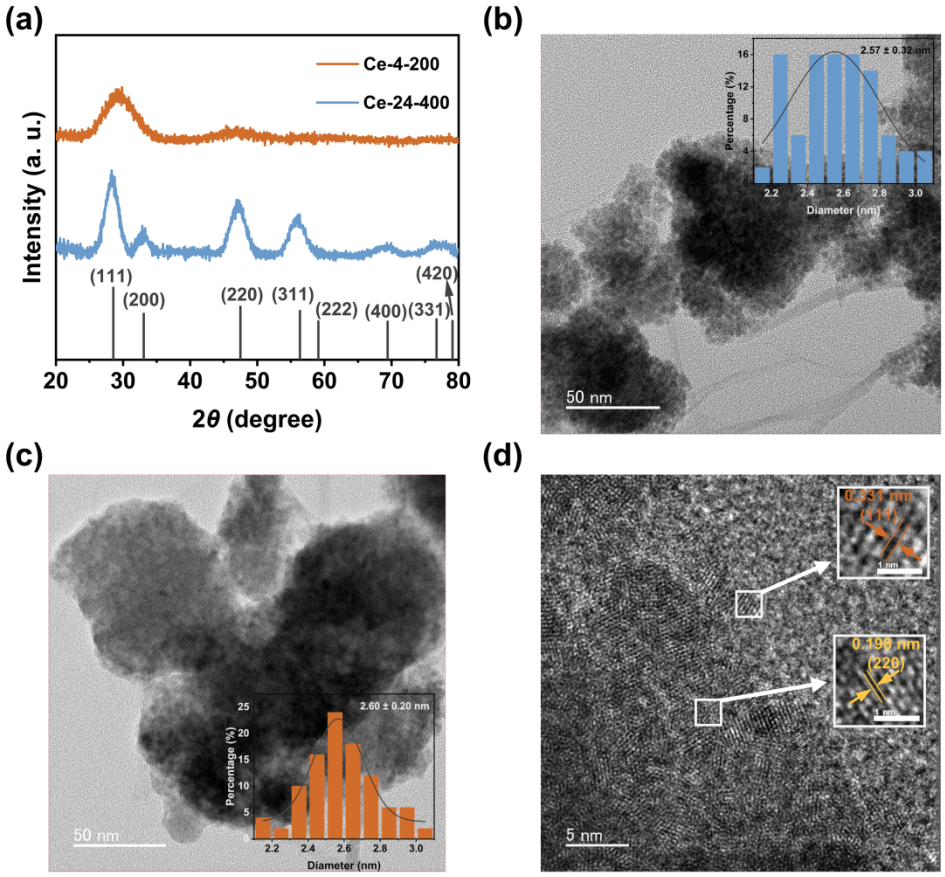

Figure S4. (a) The XRD patterns of Ce-4-200 and Ce-24-400. The TEM images (inset the size distributions) of (b) Ce-24-400, and (c) Ce-4-200. (d) The HR-TEM of Ce-4-200.

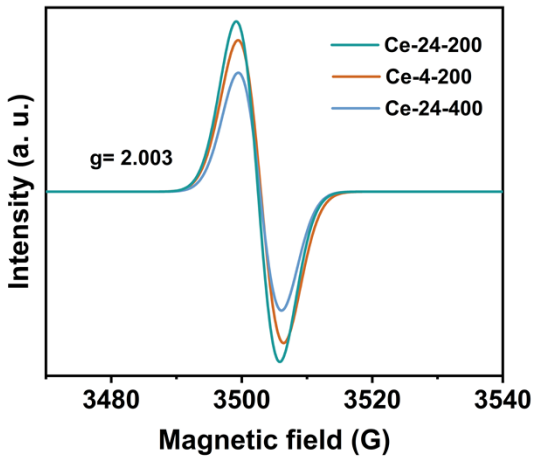

Figure S5. The EPR spectra of Ce-4-200, Ce-24-200 and Ce-24-400.

Table S1. Comparison of kinetic parameters between biosynthesized CeO_2 NPs and other nanozymes.

Materials	Substrate	K_m (mM)	Ref.
Ag@ZnS	TMB	4.22	1
Cu3/ND@G	TMB	2.59	2
$PdPt_3$	TMB	0.26	3
Pd/MMR	TMB	0.77	4
Nanoceria	TMB	0.42	31
3-CoV MMOs	TMB	0.44	5
Co-POP	TMB	0.93	6
CeO_2 NPs	**TMB**	**0.21**	**This work**

Table S2. The ratio of Ce^{3+}, O_β, and the intensity ratio of D and G band (I_D/I_G) of Ce-4-200, Ce-24-400, and Ce-24-200.

Materials	Ce^{3+} ratio (%)	O_β ration (%)	IF2g/IVo	I_D/I_G
Ce-24-200	43.32	60.17	0.58	1.08
Ce-4-200	40.11	57.17	0.34	1.13
Ce-24-400	**28.40**	**46.47**	**0.16**	**0.16**

Table S3. Comparison with the L–PA or D–PA detection results of other detection systems.

Materials	Methods	D/L–PA	Linear range (μM)	Ref.
Ag−AuNPs	Colorimetric	L–PA	5.0–80.0	7
CeO_2/Pal NSs	Colorimetric	L–PA	10–50	8
$Pc(OH)_8$-TiO_2	Colorimetric	L–PA	6–10	9
HH-MoS2 NTs	Colorimetric	D–PA	46.9–402	10
SiQDs/DTNB	Fluorescence	D–PA	1–20	11
CDs/Hg(II)	Fluorescence	D–PA	2–24	12
CeO_2 NPs	**Colorimetric**	**L–PA**	**10–500**	**This work**

Table S4. Detection of L–PA in real samples by standard addition method.

Samples	added (μM)	Detected (μM)	Recovery (%)	RSD (%)
Tape water	20	19.42	97.10	5.83
	40	39.42	98.55	3.91
	60	55.47	92.45	11.36
	100	107.13	107.13	8.85
	200	233.79	116.90	4.18
	300	303.79	101.26	8.92
Lake water	20	19.42	97.10	9.60
	40	42.38	105.96	4.40
	60	59.42	99.03	6.87
	100	104.35	104.35	9.97
	200	212.13	106.06	2.97
	300	309.35	103.12	1.43
Diluted goat	20	22.14	110.68	11.75
serum	40	44.85	112.13	1.65
	60	62.63	104.38	3.55
	100	100.46	100.46	0.96
	200	218.79	109.40	4.40
	300	296.02	98.67	2.58

Table S5. Comparison with the GSH detection results of other detection systems.

Materials	Methods	Linear range (μM)	Ref.
BTO NPs	Colorimetric	0.50–20	13
CuPd@H–C_3N_4	Colorimetric	2–40	14
CDs@ZIF-8	Colorimetric	0–100	15
CeO_2/CuO	fluorescence	2–20	16
Ag-CDs	Colorimetric	1–60	17
In_2O_3/In_2S_3	photoelectrochemical	1–100	18
CeO_2 NPs	**Colorimetric**	**9–200**	**This work**

Table S6. Detection of GSH in real samples by standard addition method.

Sample	added (μM)	Detected (μM)	Recovery (%)	RSD (%)
Glutathione Tablets	0	5.73	—	4.54
	10	16.24	103.25	5.77
	20	25.55	99.30	2.69
	40	45.82	100.20	3.45
	80	84.26	98.28	1.35
	160	165.30	99.74	0.32

REFERENCES

(1) Tian, L.; Huang, Z.; Lu, X.; Wang, T.; Cheng, W.; Yang, H.; Huang, T.; Li, T.; Li, Z. Plasmon-Mediated Oxidase-like Activity on Ag@ZnS Heterostructured Hollow Nanowires for Rapid Visual Detection of Nitrite. *Inorg. Chem.* **2023**, *62* (4), 1659–1666.

(2) Meng, F.; Peng, M.; Chen, Y.; Cai, X.; Huang, F.; Yang, L.;Liu, X.; Li, T.; Wen, X.; Wang, N.; Xiao, D.; Jiang, H.; Xia, L.; Liu, H.; Ma, D. Defect-rich graphene stabilized atomically dispersed Cu_3 clusters with enhanced oxidase-like activity for antibacterial applications. *Appl. Catal. B-Environ.* **2022**, *301*, 120826.

(3) Ma, Z.; Dong, L.; Zhang, B.; Liang, B.; Wang, L.; Ma, G.; Wang, L. Lentinan stabilized bimetallic $PdPt_3$ dendritic nanoparticles with enhanced oxidase-like property for for L-cysteine detection. *Int. J. Biol. Macromol.* **2022**, *216*, 779–788.

(4) Wang, G.; Feng, N.; Zhao, S.; Song, L.; Zhang, Y.; Tong, J.; Liu, Y.; Kang, X.; Hu, T.; Ahmad Khan, I.; Lu, K.; Wu, H.; Xie, J. Synthesis and DFT calculation of microbe-supported Pd nanocomposites with oxidase-like activity for sensitive detection of nitrite. *Food Chem.* **2024**, *434*, 137422.

(5) Wang, Y.; Chen, C.; Zhang, D.; Wang, J. Bifunctionalized novel Co-V MMO nanowires: Intrinsic oxidase and peroxidase like catalytic activities for antibacterial application. *Appl. Catal. B-Environ.* **2020**, *261*, 118256.

(6) Guo, D.; Li, C.; Liu, G.; Luo, X.; Wu, F. Oxidase Mimetic Activity of a Metalloporphyrin-Containing Porous Organic Polymer and Its Applications for Colorimetric Detection of Both Ascorbic Acid and Glutathione. *ACS Sustainable Chem. Eng.* **2021**, *9* (15), 5412–5421.

(7) Wei, J.; Guo, Y.; Li, J.; Yuan, M.; Long, T.; Liu, Z. Optically Active Ultrafine Au–Ag Alloy Nanoparticles Used for Colorimetric Chiral Recognition and Circular Dichroism Sensing of Enantiomers. *Anal. Chem.* **2017**, *89* (18), 9781–9787.

(8) Lian, J.; Liu, P.; Liu, Q. Nano-scale minerals in-situ supporting CeO_2 nanoparticles for off-on colorimetric detection of L–penicillamine and Cu^{2+} ion. *J. Hazard. Mater.* **2022**, *433*, 128766.

(9)Wang, L.; Liu, Z.; Yang, Q.; Xie, M.; Liu, Q. Sustainable Phthalocyanine-Modified TiO_2 Nanofilm as a Light-Operated Nanozyme for Colorimetric Determination of L–Penicillamine. *ACS Sustainable Chem. Eng.* **2024**, *12* (6), 2203–2211.

(10) Nazifi, M.; Ramezani, A. M.; Absalan, G.; Ahmadi, R. Colorimetric determination of D–penicillamine based on the peroxidase mimetic activity of hierarchical hollow MoS_2 nanotubes. *Sensor. Actuat. B-Chem.* **2021**, *332*, 129459.

(11) Liu, J.; Zhang, J.; Wang, M.; Su, X. Silicon quantum dots based dual-mode fluorometric and colorimetric sensing of D–penicillamine. *Talanta* **2021**, *224*, 121886.

(12) Yuan, Y.; Zhao, X.; Liu, S.; Li, Y.; Shi, Y.; Yan, J.; Hu, X. A fluorescence switch sensor used for D–Penicillamine sensing and logic gate based on the fluorescence recovery of carbon dots. *Sensor. Actuat. B-Chem.* **2016**, *236*, 565–573.

(13) Yang, D.; Liu, J.; Hu, W.; Xiao, Y.; Chen, H.; Long, Y.; Zheng, H. Nano-ferroelectric oxidase mimics for colorimetric detection of glutathione. *Sensor. Actuat. B-Chem*. **2023**, *393*, 134170.

(14) Tang, W.; An, Y.; Chen, J.; Row, K.-H. Multienzyme mimetic activities of holey CuPd@H–C_3N_4 for visual colorimetric and ultrasensitive fluorometric discriminative detection of glutathione and glucose in physiological fluids. *Talanta* **2022**, *241*, 123221.

(15) Wang, Y.; Liu, X.; Wang, M.; Wang, X.; Ma, W.; Li, J. Facile synthesis of CDs@ZIF-8 nanocomposites as excellent peroxidase mimics for colorimetric detection of H_2O_2 and glutathione. *Sensor. Actuat. B-Chem*. **2021**, *329*, 129115.

(16) Chen, W.; Chen, Y.; Shen, C.; Zhu, X.; Zhu, J.; Weng, L. Deep eutectic solvent-assisted synthesis of CeO_2/CuO nanozymes for polymer dots integrated ratiometric fluorescence detection of glutathione. *Sensor. Actuat. B-Chem*. **2024**, *414*, 135947.

(17) Lv, H.; Liu, G.; Zhang, N.; Yang, Z.; Jv, X.; Zhao, B.; Yuan, T. Ag-carbon dots with peroxidase-like activity for colorimetric and SERS dual mode detection of glucose and glutathione. *Talanta* **2024**, *273*, 125898.

(18) Liu, D.; Bai, X.; Sun, J.; Zhao, D.; Hong, C.; Jia, N. Hollow In_2O_3/In_2S_3 nanocolumn-assisted molecularly imprinted photoelectrochemical sensor for glutathione detection. *Sensor. Actuat. B-Chem*. **2022**, *359*, 131542.